Theoretical Analysis of Reverse Link Capacity for an SIR-Based Power-Controlled Cellular CDMA System in a Multipath Fading Environment

Duk Kyung Kim, *Member, IEEE,* and Fumiyuki Adachi, *Senior Member, IEEE*

Abstract—Capacity estimation in a code-division multiple-access system is closely related to power control schemes, which complicates the analysis due to the interaction between the signal power and the interference from other users and from other paths. For a signal-to-interference ratio (SIR)-based power control scheme, most previous work has been restricted to a single-cell system or to a multiple-cell system neglecting the effect of multipath fading. This paper is to give a theoretical foundation to the possible reverse link capacity of a multiple-cell system with perfect SIR-based power control, assuming two different multipath Rayleigh fading channel models: uniform and exponential power delay profiles. The effects of the numbers of resolvable propagation paths and Rake fingers, and other system parameters such as the required E_b/I_o, the processing gain, and the maximum allowable transmit power of a mobile station, are investigated. The results are compared between single- and multiple-cell systems. When the number of resolvable paths is one or the number of Rake fingers is one, the link capacity becomes zero in a multiple-cell environment. This can be avoided by the use of antenna diversity. Antenna diversity reception is found to linearly increase the link capacity as the number of antennas increases.

Index Terms—Code division multiple access (CDMA), cellular system, link capacity, power control.

I. INTRODUCTION

AFTER the first launch of analog mobile communication systems, better known as first-generation systems, there has been an explosive increase in the number of mobile users in the last two decades. Even though second-generation systems such as IS-95, GSM, and PDC are being successfully operated in many countries [1], third-generation systems called International Mobile Telecommunications-2000 (IMT-2000) are required in the near future [2]. The driving forces are higher system capacity, higher communication quality, and flexible accommodation of a variety of wide-band services with different data rates. Among them, the system capacity is a key factor to compare the performances of various mobile communication systems. Direct sequence code-division multiple access (DS-CDMA or CDMA for short) is being strongly considered as a radio interface technology for IMT-2000

systems [3]. Unlike time-division multiple-access systems, the capacity of a CDMA system is interference-limited. Many approaches such as interference cancellation, smart antenna, and fast transmit power control (TPC) are being actively studied to reduce the interference from other users and hence increase the link capacity.

Capacity is closely related to TPC schemes in CDMA systems. Many previous papers were based on strength-based fast TPC. For example, Gilhousen *et al.* [4] calculated the capacity of systems supporting voice traffic, and Ariyavisitakul [5] simulated a strength-based fast TPC system. However, the signal-to-interference ratio (SIR)-based fast TPC is employed in IMT-2000 systems as well as in IS-95 systems due to its potential for higher system performance. Different ways can be implemented to measure the received instantaneous SIR; for example, IS-95 systems can use automatic gain control (AGC) to normalize the noise variance to unity [6], but IMT-2000 systems can use the pilot symbols, which are transmitted on the reverse link [7]. This potential was indicated by Ariyavisitakul [8] using a simulation method. The sum of the interference from other users is well approximated as a Gaussian noise, when observed over a short-term time interval (which is defined as a time interval enough to remove the instantaneous channel variations due to fading but not to remove those due to shadowing), due to central limit theorem for a large number of users. So we use this approximation [15], [21], [23]. Thus, the transmission quality represented by the bit error rate (BER) can be evaluated using the signal energy per information bit-to-*short-term average* interference plus background noise power spectrum density ratio E_b/I_o. In a mobile communications system, the link capacity is often defined as the maximum number of users per base station (or radio cell) to maintain the probability that the received E_b/I_o cannot satisfy the required E_b/I_o (this is called outage) at a prescribed value. Kim and Sung [9] introduced a methodology for capacity estimation for an SIR-based power-controlled system in a multiple-cell environment and investigated the effects of the voice activity factor, the required E_b/I_o, the maximum received power, and propagation parameters on the reverse (mobile-to-base) link capacity. Kim and Sung [10] and Kim and Adachi [11] extended the above analysis to a multicode CDMA system and an overlaid multiband CDMA system, respectively. Fast TPC controls the instantaneous transmit power, so that the received E_b/I_o after Rake combining is kept at the prescribed target value. Thus, the multipath fading impacts the transmit power with fast TPC and, accordingly, other cell interference. However, in the

above theoretical works, the impact of multipath fading on the other cell interference was neglected, and was included only in the value of required E_b/I_o or target E_b/I_o.

Rake combing is a unique method of CDMA systems to combat the multipath fading [12], [13]. Various combining techniques for Rake receivers were analyzed in a multipath fading environment [14]. Kchao and Stuber [15] approximately derived the area averaged BER of a single cell system for three different combining techniques in a multipath fading environment. They also considered a multiple cell environment, where the base station (BS) was assumed to receive the same total average signal power from each mobile station (MS) [16]. Adachi [17] evaluated the achievable BER performance for an SIR-based fast TPC scheme under a multipath fading environment. However, his analysis focused on a single cell system. Adachi [18] also investigated the Rake combing effect in a multiple cell environment, where he used Monte Carlo simulations, but other cell interference was modeled based on the average interference ratio f (constant value) of the other cell and the own cell. So far, the multiple cell capacity under a multipath fading environment has not been mathematically dealt for an SIR-based fast TPC scheme, mainly because the fast TPC complicates the analysis due to the interaction between the signal power and the interference from other users and from other paths.

The purpose of this paper is to give a theoretical foundation to the possible reverse link capacities of single- and multiple-cell systems in a multipath fading environment, where the SIR-based fast TPC is performed perfectly with an M-finger Rake receiver. The theoretical investigation of the effects of the number of resolvable propagation paths and the number of Rake fingers are given assuming two different multipath Rayleigh fading channel models: uniform and exponential power delay profiles. How the numbers of paths and Rake fingers affect the link capacities of single- and multiple-cell systems differently is discussed in detail. The effects of the required E_b/I_o, the processing gain, and the maximum allowable transmit power of an MS are also discussed in this paper. In addition, antenna diversity reception is investigated.

II. MULTIPATH FADING CHANNEL MODEL

Due to the reflection by obstacles such as buildings, there are many propagation paths with different delays and different amplitudes. The multipath fading is called frequency selective if multiple resolvable paths exist. It is assumed in this paper that each resolvable propagation path suffers from the same attenuation according to the distance and the same shadowing. A DS-CDMA receiver can resolve the multipath channel into several frequency-nonselective paths with discrete delays of a multiple of chip duration T_c. The equivalent low-pass impulse response of the multipath fading channel between the MS of interest and the BS can be expressed as [15], [17]

$$h(t, \tau) = \sum_{l=0}^{\infty} \xi_l(t)\delta(\tau - \tau_l) \qquad (1)$$

where $\xi_l(t)$ and τ_l are the complex-valued path gain and time

delay of the lth path, respectively, and $\delta(x)$ is the delta function. $\xi_l(t)$ satisfies the following condition:

$$\sum_{l=0}^{\infty} E[|\xi_l(t)|^2] = 1 \qquad (2)$$

where $E[\cdot]$ denotes the ensemble average. The resolved path with a time delay of τ_l represents a group of unresolvable paths having time delays over the interval $[\tau_l - T_c/2, \tau_l + T_c/2]$. Assuming a wide sense stationary uncorrelated scattering (WSSUS) channel model, $\xi_l(t)$ can be modeled as an independent zero-mean complex Gaussian process due to the central limit theorem. Then, $|\xi_l(t)|$ follows a Rayleigh distribution and $|\xi_l(t)|^2$ is exponentially distributed [19]. Since the fading maximum Doppler frequency can in most practical cases be assumed to be very low compared to the data modulation symbol rate [17], the time dependency of the path gain is dropped hereafter and the notation ξ_l is used instead.

The multipath fading channel can be characterized by the power-delay profile. Two power-delay profiles are assumed in this paper: uniform and exponential

$$E[|\xi_l|^2] = \begin{cases} \dfrac{1}{L}, & 0 \le l \le L-1, \text{ for a} \\ & \quad \text{uniform profile} \\ (1-e^{-\epsilon})e^{-\epsilon l}, & l \ge 0, \text{ for an} \\ & \quad \text{exponential profile} \end{cases} \qquad (3)$$

where L is the total number of paths in a uniform profile. In an exponential profile, L is implicitly set at infinity and ϵ is a decay factor. If 90% of signal power can be captured on average by using from zeroth path to the $L_{90\%}$th path, $L_{90\%}$ is equal to $2.3/\epsilon$.

III. RECEIVED SIGNAL POWER AND OTHER CELL INTERFERENCE

It is assumed that multipath fading has no effect on the base station (BS) selection because a home BS is selected based on a short-term average signal power level, i.e., the instantaneous power variation due to multipath fading is removed and only the influence of shadowing and distance-dependent path loss remains (hereafter, unless otherwise stated, the term "short-term average" is dropped for simplicity). In [9]–[11], the relation between the received signal power and the other cell interference was derived for a given required E_b/I_o (the impact of multipath fading on other cell interference was neglected and was only included in the value of required E_b/I_o). The following were assumed:

1) ideal hexagonal cell structure with a unit cell radius;
2) the zeroth cell of interest and 18 other cells with index k in the first and second tiers;
3) spatially uniform density of users $\rho = (2N/3\sqrt{3})$, where N is the number of users of each cell;
4) perfect fast TPC;
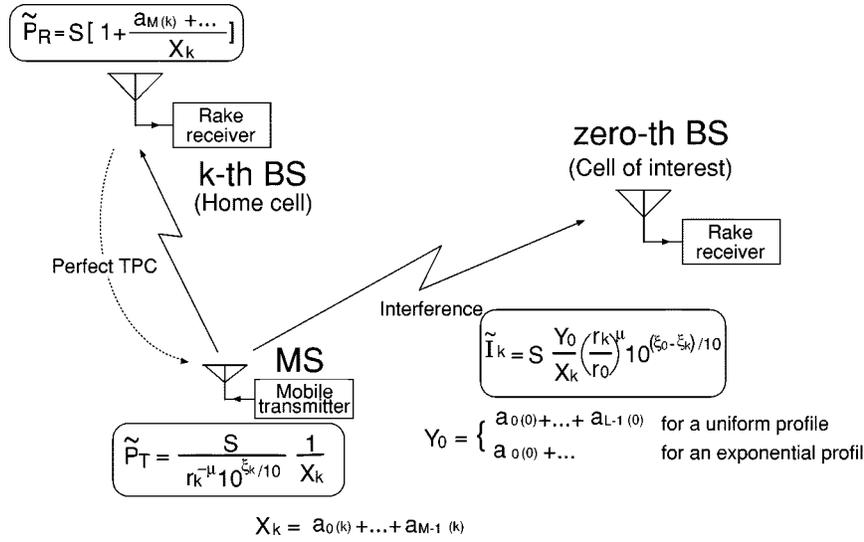5) the best cell site that has the least product of path loss and shadowing is always selected for each user to com-

Fig. 1.   The power levels at an MS, its home BS with an index k, and the zeroth BS if power control is perfect with an ideal M-finger Rake receiver.

municate with (this is equivalent to selection type of soft handoff);

6) Gaussian model for other cell interference power; hence, the distribution function can be expressed using the mean and variance.

Let μ be the path-loss exponent and the shadowing follow a log-normal process with standard deviation σ dB and mean $= 0$ dB. Then, when neglecting the impact of multipath fading, the mean m_I and variance σ_I^2 of total other cell interference power I can be approximated as [9], [10]

$$m_I \approx M(\mu, \sigma)E[S]N \qquad (4)$$
$$\sigma_I^2 \approx \{A(\mu, \sigma)E[S^2] - B(\mu, \sigma)E^2[S]\}N \qquad (5)$$

where

$E[\cdot]$ ensemble operation;
S received power.
$M(\mu, \sigma)$, $A(\mu, \sigma)$, and $B(\mu, \sigma)$ are given by

$$M(\mu, \sigma) = e^{\{\sigma \ln(10)/10\}^2} \iint \left(\frac{r_k}{r_0}\right)^{\mu} \Phi$$
$$\cdot \left(\frac{10\mu}{\sqrt{2\sigma^2}} \log_{10}(r_o/r_k) - \sqrt{2\sigma^2}\frac{\ln(10)}{10}\right) \rho' \, dA$$

$$A(\mu, \sigma) = e^{\{\sigma \ln(10)/5\}^2} \iint \left(\frac{r_k}{r_0}\right)^{2\mu} \Phi$$
$$\cdot \left(\frac{10\mu}{\sqrt{2\sigma^2}} \log_{10}(r_o/r_k) - \sqrt{2\sigma^2}\frac{\ln(10)}{5}\right) \rho' \, dA$$

$$B(\mu, \sigma) = e^{2\{\sigma \ln(10)/10\}^2} \iint \left(\frac{r_k}{r_0}\right)^{2\mu} \Phi^2$$
$$\cdot \left(\frac{10\mu}{\sqrt{2\sigma^2}} \log_{10}(r_o/r_k) - \sqrt{2\sigma^2}\frac{\ln(10)}{10}\right) \rho' \, dA.$$

r_k is the distance from an MS to the kth BS. ρ' and $\Phi(x)$ are expressed as

$$\rho' = \rho/N$$
$$\Phi(x) = \frac{1}{\sqrt{2\pi}} \int_{-\infty}^{x} e^{-y^2/2} \, dy.$$

The values $M(\mu, \sigma)$, $A(\mu, \sigma)$, and $B(\mu, \sigma)$ depend only on μ and σ. They can be numerically obtained by considering the first and second tiers. For $\mu = 4$ and $\sigma = 8$ dB, $M(4, 8) = 0.659$, $A(4, 8) = 0.223$, and $B(4, 8) = 0.04$. The effect of different values of μ and σ can be found in [9].

Now, let us consider a multipath fading environment. If taking into account the ideal fast TPC in a multipath fading environment, we need to modify (4) and (5), reflecting instantaneous variations in the path gains. The BS is assumed to have an ideal Rake receiver with M-finger, where M is less than or equal to L for a uniform profile. Fig. 1 shows the instantaneous power levels at an MS, its home BS indexed k, and zeroth BS. Let $a_{l(k)} = |\xi_{l(k)}|^2$ denote the squared path gain of the lth path to the kth BS. $a_{l(k)}$s are exponentially distributed and mutually independent for different l and k, whose means are determined only by the path index l. Without fast TPC, the instantaneous signal power $\widetilde{P}_R$ received at antenna can be represented as

$$\widetilde{P}_R = \widetilde{P}_T r^{-\mu} 10^{\xi_k/10} \left[a_{0(k)} + \cdots + a_{M(k)} + \cdots\right] \qquad (6)$$

where $\widetilde{P}_T$ denotes the transmitted signal power from an MS. The terms in square brackets denote the power variation due to multipath fading. The receiver just collects the instantaneous power from M paths by Rake combining. Therefore, the instantaneous received signal power $\widetilde{P}_{R, Rake}$ after Rake combining becomes

$$\widetilde{P}_{R, \text{Rake}} = \widetilde{P}_T r^{-\mu} 10^{\xi_k/10} \left[a_{0(k)} + \cdots + a_{M-1(k)}\right]. \qquad (7)$$

Assuming perfect TPC, the transmit power is controlled so that the instantaneous received signal power becomes the minimum power level S satisfying the received $E_b/I_o =$ the target value. Hence

$$\widetilde{P}_T r^{-\mu} 10^{\xi_k/10} \left[a_{0(k)} + \cdots + a_{M-1(k)}\right] = S \qquad (8)$$

and $\widetilde{P}_T$ is now given by

$$\widetilde{P}_T = \frac{S}{r_k^{-\mu} 10^{\xi_k/10}} \frac{1}{X_k} \qquad (9)$$
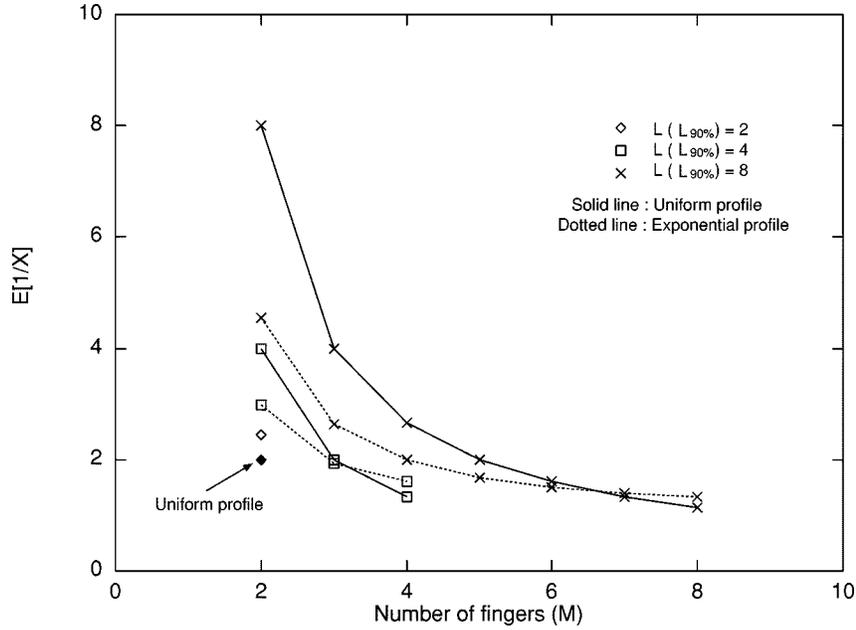
Fig. 2. $E[1/X]$ for various values of L (or $L_{90\%}$) and M for uniform and exponential profiles ($L_{90\%} = 2.3/\epsilon$).

where

$$X_k \triangleq a_{0(k)} + \cdots + a_{M-1(k)}. \qquad (10)$$

Substitution of (9) into (6) gives

$$\widetilde{P}_R = S \left[1 + \frac{a_{M(k)} + \cdots}{X_k} \right]. \qquad (11)$$

Since the instantaneous power transmitted from the MS suffers both path loss and multipath fading, the instantaneous interference power $\widetilde{I}_k$ from an MS that belongs to the kth BS to the zeroth BS can be expressed as

$$\widetilde{I}_k = S \left(\frac{r_k^\mu}{10^{\xi_k/10}} \right) \frac{1}{X_k} \left(\frac{10^{\xi_o/10}}{r_o^\mu} \right) Y_0$$

$$= S \frac{Y_0}{X_k} \left(\frac{r_k}{r_o} \right)^\mu 10^{(\xi_o - \xi_k)/10} \qquad (12)$$

where Y_0 represents the effect of multipath fading to the zeroth BS and is given by

$$Y_0 = \sum_{l=0}^{\infty} a_{l(0)}. \qquad (13)$$

Since Y_0 is independent from X_k and its expectation $E[Y_0]$ is equal to one from (2), the *short-term average* interference power I_k becomes

$$I_k = S E \left[\frac{1}{X_k} \right] \left(\frac{r_k}{r_0} \right)^\mu 10^{(\xi_o - \xi_k)/10}. \qquad (14)$$

Since X_k is independent of k, X is used instead for simplicity. As mentioned in Section II, multipath fading is assumed to have no effect on the BS selection. Moreover, Y_0 and X depend only on the type of power delay profile and the number of Rake fingers. They are independent of the location of an MS (i.e., which MS transmits the signal and which BS receives the signal). The total other cell interference power I is the sum of (14) associated with all users communicating with the kth BS for all $k > 0$. Hence, the mean m_I and variance σ_I^2 of the total other cell interference power in a multipath fading environment can be modified as

$$m_I \approx M(\mu, \sigma) E[S] E \left[\frac{1}{X} \right] N \qquad (15)$$

$$\sigma_I^2 \approx \{ A(\mu, \sigma) E[S^2] - B(\mu, \sigma) E^2[S] \} E^2 \left[\frac{1}{X} \right] N. \qquad (16)$$

m_I and σ_I^2 largely depend on L, M, and power delay profile. It should be pointed out that compared with the case of no multipath fading or neglecting the multipath fading effect [see (4) and (5)], m_I and σ_I always become larger by a factor of $E[1/X]$. Hence, the link capacity becomes smaller when the multipath fading exists due to increased other cell interference with fast TPC. This was first indicated by Adachi *et al.* in [23].

X is the sum of M exponentially distributed random variables. For a uniform profile, X is the sum of M statistically independent and identically distributed random variables and thereby has an Erlang distribution [20]

$$f_X(x) = \frac{L^M}{(M-1)!} x^{M-1} e^{-Lx} U(x) \qquad (17)$$

where $U(\cdot)$ is the step function. In this case, $E[1/X]$ is given by

$$E \left[\frac{1}{X} \right] = \frac{L}{M-1}, \qquad M \geq 2. \qquad (18)$$

On the other hand, for an exponential profile, $E[1/X]$ can be obtained numerically. Fig. 2 shows the value of $E[1/X]$ for various values of L (or $L_{90\%}$) and M for both profiles. For $M = 1$, $E[1/X]$ becomes infinite irrespective of power-delay profile shape. If M is equal to L (or $L_{90\%}$) for $M \geq 2$, the

value of $E[1/X]$ is smaller for a uniform profile than for an exponential profile because 10% power cannot be captured on average for an exponential profile. For L ($L_{90\%}$) = 8, the value of $E[1/X]$ is greatly reduced by increasing M from one to four, but the reduction is almost saturated as M increases beyond four.

IV. COMPUTATION PROCEDURE FOR REVERSE LINK CAPACITY

A. Expression for E_b/I_o After Rake Combining

Assuming an ideal Rake combiner with M-finger, the E_b/I_o of the zeroth MS of the zeroth cell is the sum of the E_b/I_o of each path and can be expressed as [15], [17]

$$\frac{E_b}{I_o} = \sum_{m=0}^{M-1} \left(\frac{E_b}{I_o}\right)_m \tag{19}$$

where $(E_b/I_o)_m$ is the E_b/I_o of mth path. Since all users' received signals on the reverse link are time asynchronous and the time delay τ_l of the lth path varies, $(E_b/I_o)_m$ is given, from (11), by [9], [10]

$$\left(\frac{E_b}{I_o}\right)_m \triangleq \frac{GS\dfrac{a_{m(0)}^{(0)}}{X_0^{(0)}}}{\dfrac{2}{3}\left\{SE\left[\displaystyle\sum_{n=0}^{N-1}\sum_{l=0}^{\infty}\dfrac{a_{l(0)}^{(n)}}{X_0^{(n)}} - \dfrac{a_{m(0)}^{(0)}}{X_0^{(0)}}\right] + I\right\} + 1} \tag{20}$$

with G being the processing gain defined as W/R, where W is the spreading code chip rate and R is the information data rate, and I being the total other cell interference power. The factor 2/3 in the denominator of (20) is due to the assumption of square chip pulse. The first term inside $\{\cdot\}$ of the denominator is the own cell interference. In (20), the signal power and interference power have been normalized by the background noise power $\eta_o W$, where $\eta_o/2$ is the two-sided background noise power spectrum density [thus, S and I are now the signal-to-noise power ratio (SNR) and the interference-to-noise power ratio (INR) at the receiver input, respectively]. $X_0^{(n)}$ represents X_0 of the nth MS and are statistically independent and identically distributed random variables. $a_{l(0)}^{(n)}$ denotes the squared path gain of the lth path from the nth MS of the zeroth cell, and its distribution depends only on the path index l. M paths are selected to have the highest power on average.

For a large number of users, $a_{m(0)}^{(0)}$ in the denominator has a negligible impact and can be omitted. Hence, substitution of (20) into (19) yields

$$\frac{E_b}{I_o} \approx \frac{GS}{\dfrac{2}{3}\left\{NS + SE\left[\displaystyle\sum_{n=0}^{N-1}\dfrac{1}{X_0^{(n)}}\sum_{l=M}^{\infty}a_{l(0)}^{(n)}\right] + I\right\} + 1}. \tag{21}$$

B. Obtaining m_I and σ_I^2

The target value of E_b/I_o is set at γ_0, and S is the minimum power level satisfying $E_b/I_o = \gamma_0$, as defined in (8). Then, S can be expressed as

$$S = \frac{I + \frac{3}{2}}{\dfrac{3}{2}\dfrac{G}{\gamma_0} - N - E\left[\displaystyle\sum_{n=0}^{N-1}\dfrac{1}{X_0^{(n)}}\sum_{l=M}^{\infty}a_{l(0)}^{(n)}\right]}$$

$$\triangleq \frac{I + \frac{3}{2}}{\dfrac{3}{2}\dfrac{G}{\gamma_0} - N(1 + D)}. \tag{22}$$

Since $a_{l(0)}^{(n)}$, $l > M$, and $X_0^{(n)}$ are mutually independent, D can be expressed as

$$D = \sum_{l=M}^{\infty} E\left[\frac{a_{l(0)}^{(n)}}{X_0^{(n)}}\right] \triangleq E\left[\frac{1}{X}\right]D_a. \tag{23}$$

For the uniform profile, D_a is given by

$$D_a \triangleq \sum_{l=M}^{\infty} E\left[a_{l(0)}^{(n)}\right] = (L - M)\frac{1}{L} \tag{24}$$

and for the exponential profile

$$D_a = e^{-\epsilon M}. \tag{25}$$

Since we are assuming that the distribution of the total other cell interference power I is Gaussian, the probability density function of I can be expressed as

$$f_I(x) = \frac{1}{\sqrt{2\pi}\,\sigma_I}\exp\left[-\frac{(x - m_I)^2}{2\sigma_I^2}\right]. \tag{26}$$

Using (26), $E[S]$ and $E[S^2]$ can be calculated from

$$E[S] = \int_{x \in \Omega} \frac{x + \frac{3}{2}}{\dfrac{3}{2}\dfrac{G}{\gamma_0} - N(1 + D)}f_I(x)\,dx \tag{27}$$

$$E[S^2] = \int_{x \in \Omega} \left(\frac{x + \frac{3}{2}}{\dfrac{3}{2}\dfrac{G}{\gamma_0} - N(1 + D)}\right)^2 f_I(x)\,dx \tag{28}$$

where

$$\Omega = \left\{x \,\middle|\, x > 0 \text{ and } 0 < \frac{x + \frac{3}{2}}{\dfrac{3}{2}\dfrac{G}{\gamma_0} - N(1 + D)} \le S_{\max}\right\}$$

and $S_{\max}$ is the allowable maximum SNR. It is very important that the received SNR be limited by $S_{\max}$ in an SIR-based fast TPC system because the system can only be stable by this limitation.

The calculation steps for m_I and σ_I^2 are as follows.

1) Calculate D from (23)–(25) and check if $1 + D < (3/2)(G/\gamma_0)(1/N)$ for a given N.
2) Set m_I and σ_I^2 at zeros.
3) Calculate $E[S]$ and $E[S^2]$ from (27) and (28).
4) Calculate m_I and σ_I^2 from (15) and (16).
5) Repeat steps 3) and 4) until the differences between old and new values of m_I and σ_I^2 are within a given bound. For numerical examples, the differences are set to be less than 1%.

C. Capacity Computation

The outage probability can be expressed as

$$P_{\text{out}} = 1 - \Pr\{0 \leq S \leq S_{\max}\}. \tag{29}$$

From (22), $\Pr\{0 \leq S \leq S_{\max}\}$ can be obtained by

$$
\begin{aligned}
&\Pr\{0 \leq S \leq S_{\max}\} \\
&= \Pr\left\{0 \leq \frac{I + \frac{3}{2}}{\frac{3}{2}\frac{G}{\gamma_0} - N(1+D)} \leq S_{\max}, I \geq 0\right\} \\
&= \Pr\left\{0 \leq I \leq S_{\max}\left(\frac{3}{2}\frac{G}{\gamma_0} - N(1+D)\right) - \frac{3}{2}\right\} \\
&= \Phi\left(\frac{S_{\max}\left(\frac{3}{2}\frac{G}{\gamma_0} - N(1+D)\right) - \frac{3}{2} - m_I}{\sigma_I}\right) \\
&\quad - \Phi\left(-\frac{m_I}{\sigma_I}\right).
\end{aligned}
\tag{30}
\tag{31}
$$

System capacity can now be obtained in terms of the admissible number of users keeping outage probability less than or equal to a threshold. This threshold can be denoted as the maximum allowable outage probability, which is set at 0.01 for numerical examples in this paper.

As a special case, let us consider a single-cell system. Since there is no other cell interference, the link capacity can be directly obtained from (22) and is given by

$$N = \frac{\frac{3}{2}\left(\frac{G}{\gamma_0} - \frac{1}{S_{\max}}\right)}{1 + D}. \tag{32}$$

For a uniform profile and when $L = M$, $D_a = 0$ from (22) and hence $D = 0$. Therefore

$$N = \frac{3}{2}\left(\frac{G}{\gamma_0} - \frac{1}{S_{\max}}\right). \tag{33}$$

Useful alternative expressions to (31)–(33) are given below. Since $S_{\max}$ is the maximum allowable SNR at the receiver input, we have

$$S_{\max} = \frac{1}{G}\frac{E_{b,\max}}{\eta_o} = \frac{\gamma_0}{G}\frac{I_{o,\max}}{\eta_o} \tag{34}$$

TABLE I
SYSTEM PARAMETERS

R	32 kbps
W	4.096 Mcps
γ_0	1.92 (2.84 dB)
$S_{\max}$	0 dB
P_{out}	0.01
μ	4
σ	8 dB

where $I_{o,\max}$ represents the allowable maximum value of interference plus background noise and $I_{o,\max}/\eta_o \geq 1$. Hence, we obtain for a multiple cell

$$
\begin{aligned}
&\Pr\{0 \leq S \leq S_{\max}\} \\
&= \Phi\left(\frac{\frac{I_{o,\max}}{\eta_o}\left(\frac{3}{2} - \frac{\gamma_0}{G}N(1+D)\right) - \frac{3}{2} - m_I}{\sigma_I}\right) \\
&\quad - \Phi\left(-\frac{m_I}{\sigma_I}\right)
\end{aligned}
\tag{35}
$$

and for a single cell

$$N = \frac{\frac{3}{2}\frac{G}{\gamma_0}\left(1 - \frac{\eta_o}{I_{o,\max}}\right)}{1 + D}. \tag{36}$$

Equation (35) is used to compute the capacity of a multiple-cell system. Equation (36) represents the capacity of a single-cell system. As $I_{o,\max}/\eta_o$ increases, the link approaches the interference-limited condition.

V. NUMERICAL EXAMPLES

Table I shows the system parameters, which are based on the specification of IMT-2000 systems. For the numerical computation of the link capacity, the E_b/I_o target is necessary. To obtain the E_b/I_o target for acquiring BER = 10^{-3}, an SIR-based fast power-controlled reverse link with convolutional coding of rate 1/3 and interleaving length of 10 ms was computer simulated in a Rayleigh fading environment with Vehicular-B power-delay profile [22]. It was found from our computer simulation that an E_b/I_o target value $\gamma_0 = 2.84$ dB is required to achieve BER = 10^{-3}. Propagation parameters $\mu = 4$ and $\sigma = 8$ dB are assumed. These parameters are used in this paper unless otherwise stated.

A. Single-Cell Case

Fig. 3 shows the link capacity for both profiles in a single-cell environment for varying the values of L (or $L_{90\%}$) and M. When M is equal to L for a uniform profile, link capacity is the same irrespective of L because $D = 0$ and $I = 0$ always in (22). For an exponential profile, the capacity becomes zero for $M = 1$ because of the impact of the infinite value of $E[1/X]$ on D ($D \neq 0$ in this case). For $M \geq 2$, the capacity at $M = L_{90\%}$ increases as $L_{90\%}$ increases due to the reduction in D and $E[1/X]$. When $M = L$ (or $L_{90\%}$) = 8, the capacity for an exponential profile is approximately 87% of the capacity for a uniform profile.
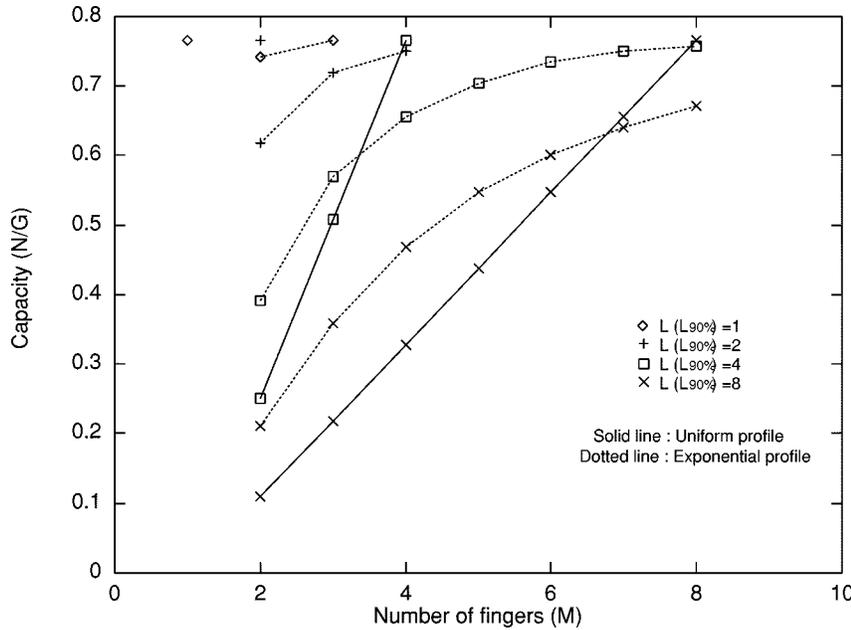
Fig. 3.   The link capacity for various values of L (or $L_{90\%}$) and M for uniform and exponential profiles in a single-cell environment.
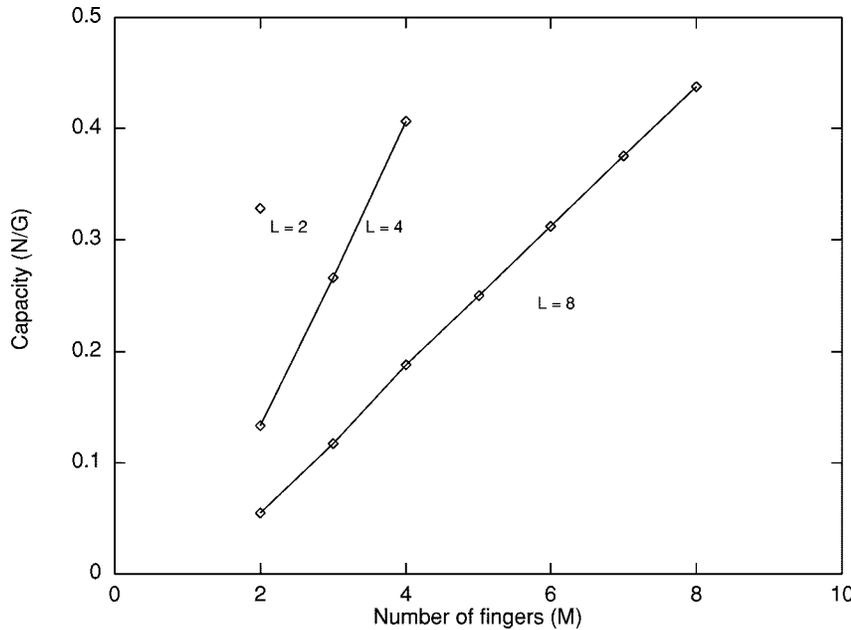

Fig. 4.   The link capacity for various values of L and M for a uniform profile in a multiple-cell environment.

To achieve the same amount of capacity for a uniform profile, more than $2L_{90\%}$ Rake fingers are required for an exponential profile. According to the profiles, different trends are observed by varying the value of M for the same value of L (or $L_{90\%}$). For an exponential profile, since additional power to be captured becomes smaller by adding a path with a longer path delay, the capacity increase tends to be saturated as M increases. On the other hand, the same power can be captured on average in each path for a uniform profile. Hence, the capacity tends to increase linearly as M increases. It is interesting to note that the single-cell capacity for $M = L$ for a uniform profile is the same as the capacity when the impact of multipath fading is ignored, which can be easily expected from (22)–(24).

B. Multiple-Cell Case

Fig. 4 shows the link capacity for a uniform profile in a multiple-cell environment. As shown in (15) and (16), the mean and the variance of total other cell interference depend on the number M of Rake fingers. For $M = 1$, the infinite value of $E[1/X]$ causes the link capacity to be zero even when $M = L$ because the other cell interference power becomes infinite. As more paths are used for a Rake receiver, the value of $E[1/X]$ can be reduced but saturated, as shown in Fig. 2. Therefore, for $M = L$, as L increases, the capacity can be increased but saturated and approaches more closely to the capacity of the case when the impact of fading is neglected. For $M = L = 8$, the capacity is approximately 57% of the single-cell capacity. (It was
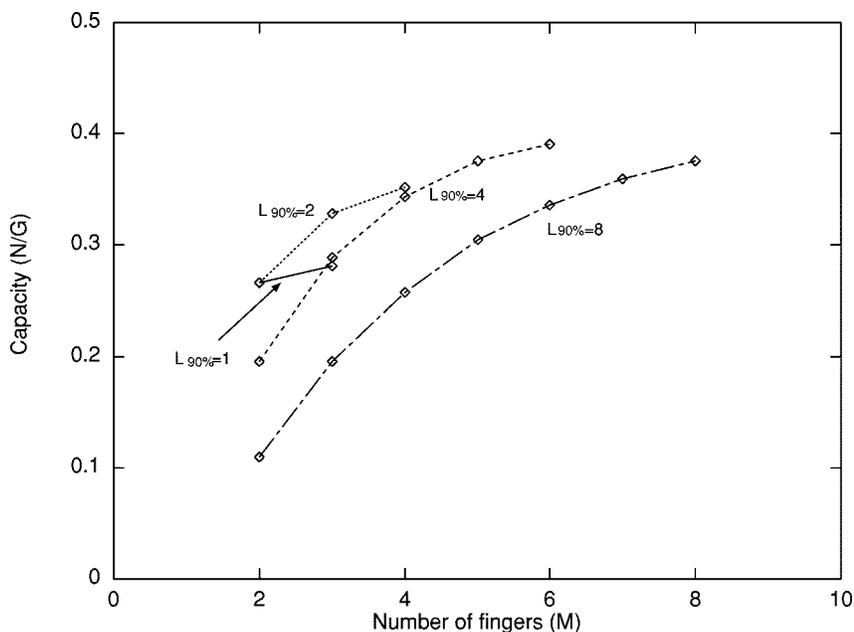
Fig. 5. The link capacity for various values of $L_{90\%}$ and M for an exponential profile in a multiple-cell environment.

found that the multiple-cell capacity is approximately 60% of the single-cell capacity when neglecting the impact of the multipath fading on fast TPC [9], [10]. This agrees with our numerical result.)

Fig. 5 shows the capacity for an exponential profile in a multiple-cell environment. Similar trends as in a single-cell environment can be observed for a same value of $L_{90\%}$. The capacity in the case of $M = L_{90\%} = 8$ is approximately 57% of the single-cell capacity (see Fig. 4) and is approximately 86% of that for a uniform profile (see Fig. 4). It is found that multiple-cell capacities in this paper for both uniform and exponential profiles are mostly consistent with the previous simulation results in [18].

C. Comparison Between Single and Multiple-Cell Cases

The multiple-cell capacity has a different trend from the single-cell capacity according to the numbers of paths and fingers. Table II compares the system capacities for various numbers of paths when $M = L$ for a uniform profile. The multiple-cell capacity becomes zero when $M = 1$, as indicated in the previous subsection. Thus, when $L = 1$, intentionally added multipaths or antenna diversity reception should be used to avoid null capacity, which occurs because the value of $E[1/X]$ becomes infinite and therefore, the other cell interference power becomes infinite, as mentioned in Section V-B. The effect of antenna diversity reception will be investigated in the following section.

Table III shows a different trend of single-cell capacity for the case of exponential profile when $M = L_{90\%}$. Unlike the case of uniform profile, single-cell capacity is also influenced by $E[1/X]$, which has already been illustrated in Fig. 3.

D. Impact of the Target Value γ_0 of Fast TPC

Fig. 6 investigates the effect of γ_0, where the single- and multiple-cell capacities are obtained for both profiles. It can be un-

TABLE II
THE SYSTEM CAPACITIES IN SINGLE- AND MULTIPLE-CELL ENVIROMNENTS
WHEN $M = L$ FOR A UNIFORM PROFILE

L	1	2	4	8
Single	0.77	0.77	0.77	0.77
Multiple	0.0	0.33	0.41	0.44
$\frac{\text{Multiple}}{\text{Single}}$	0 %	43 %	53 %	57 %

TABLE III
SYSTEM CAPACITIES IN SINGLE- AND MULTIPLE-CELL ENVIROMENTS WHEN
$M = L_{90\%}$ FOR AN EXPONENTIAL PROFILE

$L_{90\%}$	1	2	4	8
Single	0.0	0.62	0.66	0.67
Multiple	0.0	0.27	0.34	0.38
$\frac{\text{Multiple}}{\text{Single}}$	—	44 %	52 %	57 %

derstood that from (33), the link capacity is inversely proportional to γ_0. Since the effect $W\eta_o$ on link capacity is negligible, the effect of G can be estimated from these results. Doubling the value of γ_0 is equivalent to decreasing the value of G by half in view of link capacity.

E. Impact of the Transmit Power Limitation

So far, only the received power is assumed to be limited and the transmit power of an MS is assumed to be infinite. In a practical system, the transmit power is limited. Below, the SNR equivalent to the maximum transmit power is assumed to be 130 dB. Then, the link capacity varies according to the coverage size of each BS (or cell size). For example, let us consider a special case where $M = L$ for a uniform profile in a single-cell envi-
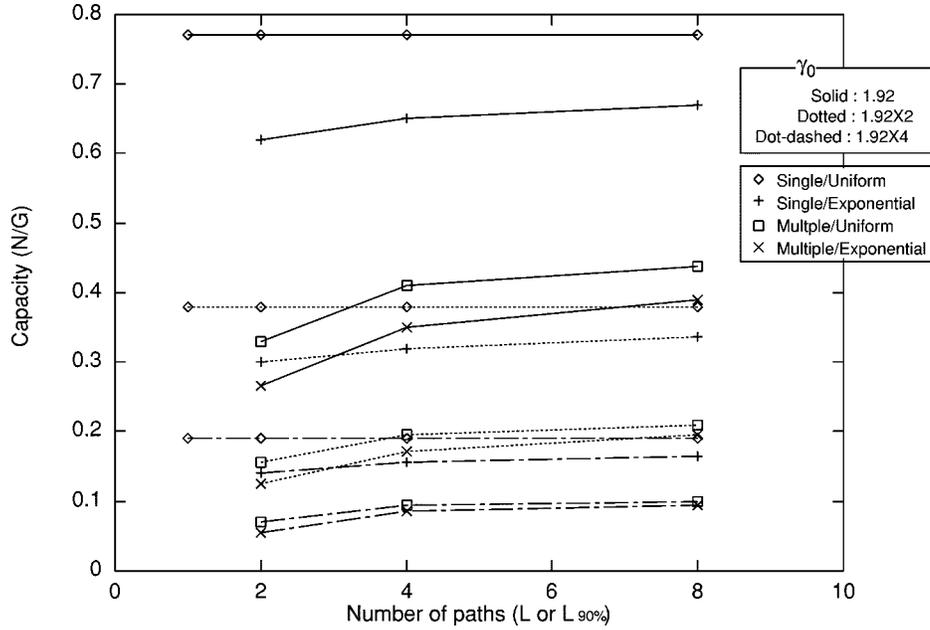
Fig. 6. The link capacity for varying the value of γ_0 for $M = L$ (or $L_{90\%}$).

ronment. Since $D = I = 0$ and from (9) and (22), the instantaneous transmit SNR at an MS can be expressed as

$$\widetilde{P}_T = \left(\frac{\frac{3}{2}}{\frac{3}{2}\frac{G}{\gamma_0} - N} \right) \frac{1}{r^{-\mu}10^{\xi/10}} \frac{1}{X}. \tag{37}$$

Assuming a circular cell with a radius of R and a uniform distribution of users for simplicity, the link capacity can be expressed by

$$\text{Capacity} = \int_0^R \text{(link capacity when users are located at } r$$
$$\frac{2\pi r}{\pi R^2} dr$$
$$\triangleq \int_0^R C_r \frac{2r}{R^2} dr \tag{38}$$

where C_r can be obtained as the maximum value of N satisfying

$$\text{Pr}\{\widetilde{P}_T > 130\,\text{dB}\} = 0.01.$$

Fig. 7 shows the link capacity for various values of the cell size R and the number of paths L. The link capacity largely depends on the distance and drastically varies in the range of $L < 4$. If the transmit power of an MS is limited in an SIR-based fast TPC system, the user around the cell boundary cannot meet the required E_b/I_o more frequently than the user near the BS receiver. Therefore, as the cell becomes larger, the total link capacity reduces when the transmit power of an MS is limited.

VI. ANTENNA DIVERSITY RECEPTION

Let us consider a uniform profile. Since $M \leq L$ and $E[1/X] = L/(M-1)$ from (18), the value of $[1/X]$ becomes infinite if $L = 1$. This means that the multiple-cell capacity becomes zero if $L = 1$, as discussed in the previous section. This is also true for the exponential profile. To avoid this situation, we need to adopt antenna diversity in the multiple-cell system using a narrow-band CDMA, where the number of resolvable paths is one at a high probability.

A. Received Signal Power and Other Cell Interference

When J-branch antenna diversity is used, J number of M-finger Rake combiner outputs, each associated with different antennas, are just combined (this is equivalent to JM-finger Rake receiver). It can be understood from this observation that when J-branch antenna diversity is used, the instantaneous transmit power is expressed by (9) by replacing X_k with

$$X_k' \triangleq \sum_{j=0}^{J-1}\sum_{m=0}^{M-1} a_{j,m(k)} \tag{39}$$

where $a_{j,m(k)}$ is the square path gain of the mth path to the kth BS experienced on the jth antenna. The instantaneous received signal power on the jth antenna, corresponding to (11), is expressed as

$$\widetilde{P}_{R,j} = S\frac{Y_0'}{X_k'} \tag{40}$$

where

$$Y_0' \triangleq \sum_{l=0}^{\infty} a_{j,l(0)}. \tag{41}$$

Since Y_0' is independent of X_k' and its expectation $E[Y_0'] = 1$, the mean m_I and variance σ_I^2 of the total other cell interference power in a multipath fading environment with antenna diversity reception are obtained from (15) and (16), respectively, by replacing X_k with (39).
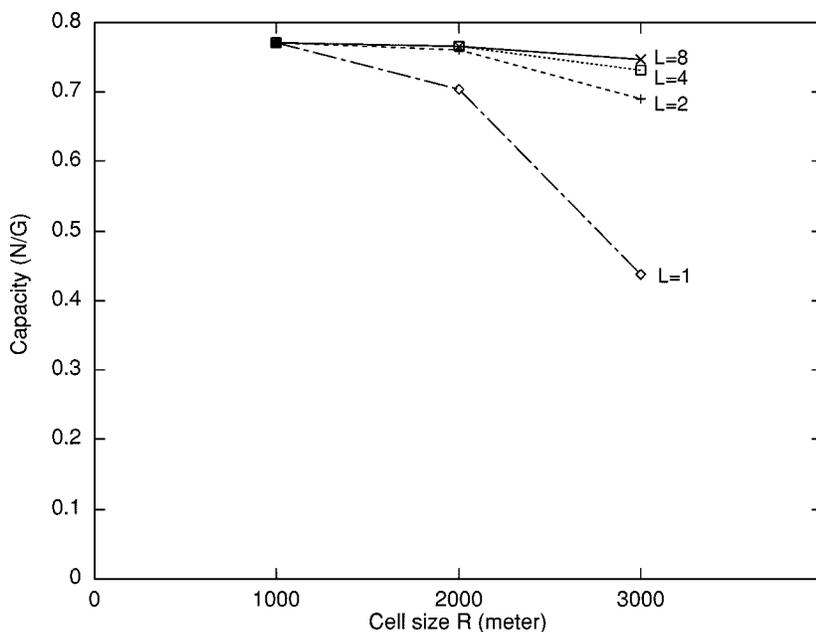
Fig. 7. The link capacity for varying the cell size R when $M = L$ for a uniform profile in a single cell environment (maximum of transmit power $= 130$ dB).
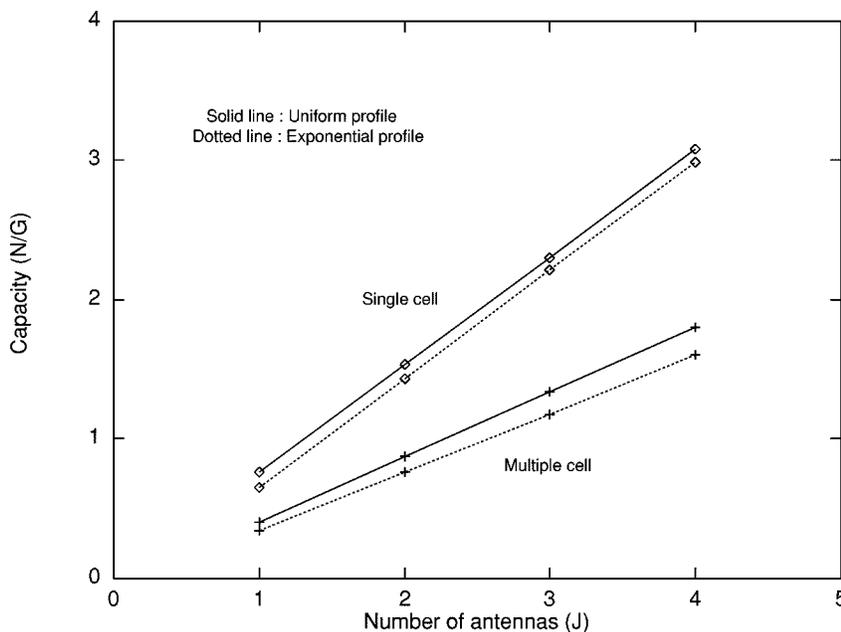

Fig. 8. The link capacity for varying the value of J for $M = L$ (or $L_{90\%}) = 4$.

Let us obtain $E[1/X']$ for the case of uniform profile. For J uncorrelated antennas (i.e., $a_{j, m(k)}$s are mutually independent for different j and m), $f_{X'}(x)$ is obtained by simply letting $M \to JM$ in (17) and is given by

$$f_{X'}(x) = \frac{L^{JM}}{(JM - 1)!} x^{JM-1} e^{-Lx} U(x). \qquad (42)$$

Thus, we can obtain

$$E\left[\frac{1}{X'}\right] = \frac{L}{JM - 1}. \qquad (43)$$

From (43), even when $M = L = 1$, $E[1/X']$ does not become infinite if $J \geq 2$. Furthermore, when $M = L$, $E[1/X']$ becomes

$$E\left[\frac{1}{X'}\right] \to \frac{1}{J}, \qquad \text{for large } L.$$

This means that the average interference power can be reduced by a factor of J, thereby increasing the capacity J times. For the exponential profile, the value of $E[1/X']$ can be obtained numerically.

B. Capacity Computation

The E_b/I_o of the zeroth MS of the zeroth cell is the sum of the E_b/I_o of each path for all antennas. Corresponding expressions to (19) and (20) are given by

$$\frac{E_b}{I_o} = \sum_{j=0}^{J-1} \sum_{m=0}^{M-1} \left(\frac{E_b}{I_o} \right)_{j,m} \tag{44}$$

$$\left(\frac{E_b}{I_o} \right)_{j,m}$$
$$\triangleq \frac{GS \frac{a_{j,m(0)}^{(0)}}{X_0^{'(0)}}}{\frac{2}{3} \left\{ SE \left[\sum_{n=0}^{N-1} \sum_{l=0}^{\infty} \frac{a_{j,l(0)}^{(n)}}{X_0^{'(n)}} - \frac{a_{j,m(0)}^{(0)}}{X_0^{'(0)}} \right] + I \right\} + 1} \tag{45}$$

where

$$X_0^{'(n)} = \sum_{j=0}^{J-1} \sum_{m=0}^{M-1} a_{j,m(0)}^{(n)}. \tag{46}$$

For a large number of users, $a_{j,m(0)}^{(0)}$ in the denominator of (45) has a negligible impact and can be omitted. Since $E[\sum_{l=0}^{\infty} a_{j,l(0)}^{(n)}/X_0^{'(n)}]$ is independent of n and j, (44) can be approximated as

$$\frac{E_b}{I_o} \approx \frac{GS}{\frac{2}{3} \left\{ SNE \left[\sum_{l=0}^{\infty} \frac{a_{,l(0)}^{(n)}}{X_0^{'(n)}} \right] + I \right\} + 1}. \tag{47}$$

Since $\sum_{l=0}^{\infty} a_{j,l(0)}^{(n)} = \sum_{l=0}^{M-1} a_{j,l(0)}^{(n)} + \sum_{l=M}^{\infty} a_{j,l(0)}^{(n)}$ and letting $X_{j(0)}^{'(n)} = \sum_{l=0}^{M-1} a_{j,l(0)}^{(n)}$, we obtain

$$E \left[\sum_{l=0}^{\infty} \frac{a_{j,l(0)}^{(n)}}{X_0^{'(n)}} \right] = E \left[\frac{X_{j(0)}^{'(n)}}{\sum_{j'=0}^{J-1} X_{j'(0)}^{'(n)}} \right] + D' \tag{48}$$

where $D' = E[1/X']D_a$ and D_a is given by (24) and (25) for the uniform profile and the exponential profile, respectively. Furthermore, since $X_{j(0)}^{'(n)}$s for $j = 0, 1, \ldots, J-1$ are mutually independent

$$E \left[\frac{X_{j(0)}^{'(n)}}{\sum_{j'=0}^{J-1} X_{j'(0)}^{'(n)}} \right]$$

is the same for all j and n. Hence, from

$$\sum_{j=0}^{J-1} E \left[\frac{X_{j(0)}^{'(n)}}{\sum_{j'=0}^{J-1} X_{j'(0)}^{'(n)}} \right] = E \left[\frac{\sum_{j=0}^{J-1} X_{j(0)}^{'(n)}}{\sum_{j'=0}^{J-1} X_{j'(0)}^{'(n)}} \right] = 1 \tag{49}$$

we obtain

$$E \left[\frac{X_{j(0)}^{'(n)}}{\sum_{j'=0}^{J-1} X_{j'(0)}^{'(n)}} \right] = \frac{1}{J} \qquad \text{for all } n. \tag{50}$$

As a consequence, (47) becomes

$$\frac{E_b}{I_o} \approx \frac{GS}{\frac{2}{3} \left\{ SN \left(\frac{1}{J} + D' \right) + I \right\} + 1}. \tag{51}$$

The target value of E_b/I_o is set at γ_0, and S is the minimum power level satisfying $E_b/I_o = \gamma_0$, as defined in (8). Then S can be expressed as

$$S = \frac{I + \frac{3}{2}}{\frac{3}{2} \frac{G}{\gamma_0} - N \left(\frac{1}{J} + D' \right)} \tag{52}$$

which corresponds to (22) of no antenna diversity case.

Using the same procedure described in Section IV, the values of m_I and σ_I^2 are obtained. Finally, the outage probability can be calculated from

$$P_{\text{out}} = 1 - \Pr\{0 \le S \le S_{\max}\}$$

with

$$\Pr\{0 \le S \le S_{\max}\}$$
$$= \Phi \left(\frac{S_{\max} \left(\frac{3}{2} \frac{G}{\gamma_0} - N \left(\frac{1}{J} + D' \right) \right) - \frac{3}{2} - m_I}{\sigma_I} \right)$$
$$- \Phi \left(-\frac{m_I}{\sigma_I} \right). \tag{53}$$

In the case of a single-cell system, there is no other cell interference. The link capacity can be directly obtained from (52) and is given by

$$N = \frac{\frac{3}{2} \left(\frac{G}{\gamma_0} - \frac{1}{S_{\max}} \right)}{\frac{1}{J} + D'}. \tag{54}$$

For a uniform profile and when $M = L$, $D_a = 0$ and hence $D' = 0$. Therefore

$$N = \frac{3}{2}\left(\frac{G}{\gamma_0} - \frac{1}{S_{\max}}\right) J$$
$$= J N_{\text{no diversity}}. \tag{55}$$

The use of antenna diversity increases the capacity J times compared to the no antenna diversity case. This is also true in the multiple-cell case.

C. Numerical Examples

Fig. 8 shows the single- and multiple-cell capacities for various values of J when $M = L$ (or $L_{90\%}$) $= 4$. Both capacities linearly increase as J increases. Single- and multiple-cell capacities have slightly different trends according to the power-delay profile. For a single-cell case, from (55), the capacity is exactly proportional to J for a uniform profile. On the other hand, for an exponential profile, $D' \neq 0$ and D' is reduced as J increases. Hence, from (54), the capacity is increased more than just J times for an exponential profile.

The multiple-cell capacity for an exponential profile is 84~89% of that for a uniform profile; hence, the slopes are different for uniform and exponential profiles. The percentage slightly differs according to the number J of antennas because of the different impact of $E[1/X']$ on D' and other cell interference. It slightly increases but saturates as J increases. Similar trends are observed for single- and multiple-cell cases.

VII. CONCLUSION

The reverse link capacity was theoretically evaluated for a CDMA system in a multipath fading environment. Ideal Rake combining was assumed for a BS receiver, and two different power-delay profiles were considered for modeling the multipath fading channel: uniform and exponential profiles. The multiple-cell capacity differs from the single-cell capacity according to the numbers of resolvable propagation paths and Rake fingers and the power-delay profile. In a single-cell environment, the link capacity is independent of the number of paths L when $M = L$ for a uniform profile and is the same as neglecting the impact of multipath fading. On the other hand, the capacity for $M = L_{90\%}$ for an exponential profile varies according to $L_{90\%}$. To achieve the same amount of capacity as that for a uniform profile, more than $2L_{90\%}$ fingers are required for an exponential profile. In a multiple-cell environment, the capacity for $M = L$ (or $L_{90\%}$) can be increased but saturated by increasing the number of paths. When $M = L$ (or $L_{90\%}$) $= 8$, the multiple-cell capacity is approximately 57% of the single-cell capacity for both profiles, and the multiple-cell capacity for an exponential profile is approximately 86% of that for a uniform profile. The capacity is found to be inversely proportional to γ_0 and vary according to the cell size if there is a limitation on the transmit power of an MS.

When the number of resolvable paths is one or the number of Rake fingers is one, the link capacity becomes zero especially in a multiple-cell environment because of the infinite value of $E[1/X]$. This can be avoided by using antenna diversity reception, which was found to linearly increase the link capacity as the number of antennas increases.

In this paper, the impact of multipath fading during soft handoff was not considered, which may affect $E[1/X]$ and, accordingly, system performance. This impact is left for further study.

REFERENCES

[1] *IEEE Commun. Mag. (Special Issue on Wireless Personal Communications)*, vol. 33, Jan. 1995.
[2] *IEEE Personal Commun. (Special Issue on IMT-2000: Standard Efforts of the ITU)*, vol. 4, Aug. 1997.
[3] *IEEE Commun. Mag. (Special Issue on Wideband CDMA)*, vol. 36, Sept. 1999.
[4] K. S. Gilhousen, I. M. Jacobs, R. Padovani, A. J. Viterbi, L. A. Weaver Jr., and C. E. Wheatley III, "On the capacity of a cellular CDMA system," *IEEE Trans. Veh. Technol.,*, vol. 40, pp. 303–312, May 1991.
[5] S. Ariyavisitakul, "Signal and interference statistics of a CDMA system with feedback power control," *IEEE Trans. Commun.*, vol. 41, pp. 1626–1634, Nov. 1993.
[6] A. J. Viterbi, A. M. Viterbi, and W. Zehabi, "Performance of power-controlled wideband terrestrial digital communication," *IEEE Trans. Commun.*, vol. 41, pp. 559–569, Apr. 1993.
[7] S. Seo, T. Dohi, and F. Adachi, "SIR-based transmit power control of reverse link for coherent DS-CDMA mobile radio," *IEICE Trans. Commun.*, vol. E81-B, pp. 1508–1516, July 1998.
[8] S. Ariyavisitakul, "Signal and interference statistics of a CDMA system with feedback power control—Part II," *IEEE Trans. Commun.*, vol. 42, pp. 579–605, Feb./Mar./Apr. 1994.
[9] D. K. Kim and D. K. Sung, "Capacity estimation for an SIR-based power-controlled CDMA system supporting ON-OFF traffic," IEEE Trans. Veh. Technol., to be published.
[10] ——, "Capacity estimation for a multi-code CDMA system with SIR-based power control," *IEEE Trans. Veh. Technol.*, vol. 49, no. 4, 2000.
[11] D. K. Kim and F. Adachi, "Capacity estimation for overlaid multiband CDMA systems with SIR-based power control," *IEICE Trans. Commun.*, vol. E83-B, no. 7, pp. 1454–1464, July 2000.
[12] F. Adachi, A. Sawahashi, and H. Suda, "Wideband DS-CDMA for next-generation mobile communications systems," *IEEE Commun. Mag.*, pp. 56–69, Sep. 1998.
[13] F. Adachi, A. Sawahashi, and H. Suda, "Promising techniques to enhance radio link performance of wideband wireless access based on DS-CDMA," *IEICE Trans. Fundamen.*, vol. E81-A, pp. 2242–2250, Nov. 1998.
[14] K. Cheun, "Performance of direct-sequence spread-spectrum RAKE receivers with random spreading sequences," *IEEE Trans. Commun.*, vol. 45, pp. 1130–1143, Sept. 1997.
[15] C. Kchao and G. L. Stuber, "Analysis of a direct-sequence spread-spectrum cellular radio system," *IEEE Trans. Commun.*, vol. 41, pp. 1507–1516, Oct. 1993.
[16] G. L. Stuber and C. Kchao, "Analysis of a multiple-cell direct-sequence CDMA cellular mobile radio system," *IEEE J. Select. Areas Commun.*, vol. 10, pp. 669–679, May 1992.
[17] F. Adachi, "Transmit power efficiency of fast transmit power controlled DS-CDMA reverse link," *IEICE Trans. Fundamen.*, vol. E80-A, pp. 2420–2428, Dec. 1997.
[18] ——, "Rake combining effect on link capacity and peak transmit power of power-controlled reverse link of DS-CDMA cellular mobile radio," *IEICE Trans. Commun.*, vol. E80-B, pp. 1547–1555, Oct. 1997.
[19] J. G. Proakis, *Digital Communications*, 3rd ed. New York: McGraw-Hill, 1995.
[20] A. Papoulis, *Probability, Random Variables, and Stochastic Processes*, 3rd ed: McGraw-Hill, 1991.
[21] E. Geraniotis and B. Ghaffari, "Performance of binary and quaternary direct-sequence spread-spectrum multiple-access systems with random signature sequences," *IEEE Trans. Commun.*, vol. 39, pp. 713–724, May 1991.
[22] A. Shibutani, H. Suda, and F. Adachi, "Multi-stage interleaver for turbo codes in DS-CDMA mobile radio," in *Proc. APCC/ICCS*, Singapore, Nov. 23–27, 1998, pp. 391–395.
[23] F. Adachi, K. Ohno, A. Higashi, T. Dohi, and T. Okumura, "Coherent multicode DS-CDMA mobile radio access," *IEICE Trans. Commun.*, vol. E79-B, pp. 1316–1325, Sept. 1996.

Duk Kyung Kim (S'93–M'00) received the B.S degree in electrical engineering from Yonsei University, Seoul, Korea, in 1992 and the M.S. and Ph.D. degrees from the Korea Advanced Institute of Science and Technology in 1994 and 1999, respectively.

He worked at the Wireless Laboratories, NTT DoCoMo, Inc., Japan, as a Postdoctoral Researcher during 1999/2000. He was interested in asynchronous transfer mode (ATM) network and ATM-based personal communication service (PCS) networks. His research interests now include system performance analysis, soft handoff modeling, handoff management, power control, and multimedia provision in CDMA systems and medium access control for next-generation wireless systems.

Fumiyuki Adachi (M'79–SM'90) received the B.S. and Dr. Eng. degrees in electrical engineering from Tohoku University, Sendai, Japan, in 1973 and 1984, respectively.

In 1973, he joined the Electrical Communications Laboratories of Nippon Telegraph & Telephone Corporation (now NTT) and conducted various research related to digital cellular mobile communications. From 1992 to 1999, he was with NTT Mobile Communications Network, Inc., where he led a research group on wide-band/broad-band CDMA wireless access for IMT-2000 and beyond. Since January 2000, he has been with Tohoku University, Sendai, Japan, where he is a Professor in the Department of Electrical Communications at the Graduate School of Engineering. His research interests are in CDMA and TDMA wireless access techniques, CDMA spreading code design, Rake receivers, transmit/receive antenna diversity, adaptive antenna arrays, bandwidth-efficient digital modulation, and channel coding, with particular application to broadband wireless communications systems. During academic year 1984/1985, he was a United Kingdom SERC Visiting Research Fellow in the Department of Electrical Engineering and Electronics, Liverpool University. From April 1997 to March 2000, he was a Visiting Professor at Nara Institute of Science and Technology, Japan. He has written chapters of three books.

Dr. Adachi was a Corecipient of the IEICE TRANSACTIONS Best Paper of the year award in 1996 and 1998. He was a corecipient of the IEEE TRANSACTIONS ON VEHICULAR TECHNOLOGY Best Paper of the year award in 1980 and 1990.